Time-Resolved Optical Characterization of Proximized Nano-Bilayers for Ultrafast Photodetector Applications

L. Parlato(1), G. P. Pepe(1), D. Pan(2), C. De Lisio(1), V. Pagliarulo(1), A. Cosentino(1), N. Marrocco(1), D. Dalena(1), G. Peluso(1), A. Barone(1) and R. Sobolewski(2).

(1) CNR-INFM Coherentia and Università di Napoli “Federico II,” Dip. Scienze Fisiche, c/o
Fac. Ingegneria, Piazzale Tecchio 80 – 80125 Napoli, Italy

(2) Department of Electrical and Computer Engineering and the Laboratory for Laser
Energetics, University of Rochester, Rochester, New York 14627-0231

Corresponding author: e-mail: parlato@na.infn.it

Abstract **- Time-resolved transient pump-probe spectroscopy measurements on proximized ferromagnet/superconductor (F/S) structures are presented. We focused our attention on both low and high critical temperature superconductors such as Nb and YBCO, while for F the weak-ferromagnetic alloy $Ni_{0.48}Cu_{0.52}$ has been used. Dynamics of the electron-phonon relaxation process has been investigated as a function of both the temperature and the F-film thickness. In the case of NiCu/Nb bilayers a thin F overlayer reduces the bolometric component of the photoresponse, while in YBCO structures with NiCu faster relaxation times were measured. F/S nanobilayers are very attractive for the development of novel hybrid superconducting photodetectors.**

Manuscript received November 28, 2007; accepted December 21, 2007. Reference No. ST20, Category 4.
Paper submitted to Proceedings of EUCAS 2007; published in JPCS **98** (2008), paper # 012317

I. INTRODUCTION

Superconductors show a high potential for many radiation detection applications due to their high-energy sensitivity over a very wide frequency range (from X-ray to millimeter wavelengths), ultra-fast electronic response times (down to few ps), and radiation hardness.

In a superconductor, the response to the radiation after the absorption of radiation quanta involves a complex dynamics which depends on the relaxation processes involving phonons, quasiparticles, and Cooper pairs. At the very early stage of the cascade, the absorbed energy E_0 is conveyed to a fast photoelectron, and the down-conversion process is dominated by electron-electron (*e-e*) scattering. A nonequilibrium hot electron-hole distribution occurs typically on a time scale ≤ 10 fs, when the electron-phonon (*e-ph*) scattering process becomes mostly effective leading to the production of a large number of phonons. The time evolution of both phonon and quasiparticle distribution functions can be described by a system of coupled microscopic kinetic equations [1]. However, at $T \leq T_c$, where T_c is the superconductor critical temperature, and under weak perturbations, one can assume that the electron and phonon dynamics are described in terms of their energy distributions: two different temperatures T_e and T_{ph} can be assigned to the electron and phonon sub-systems. The nonequilibrium state is hence described by a system of two coupled differential time-dependent energy-balance equations [2], commonly referred as the two-temperature model (2-T). The 2-T equations involve the e-ph coupling constant $g_{e\text{-}ph}$, the external source term (*e.g.*, the optical pump pulse), and the heat capacities of both electrons and phonons, C_e and C_{ph}. At low excitation fluencies and/or near T_c, the temperature dependences of C_e, C_{ph}, and $g_{e\text{-}ph}$ can be neglected and the e-ph relaxation time can be simplified as $\tau_{e\text{-}ph} = C/g_{e\text{-}ph}$, where $1/C = 1/C_{el} + 1/C_{ph}$. The estimation of C_e, C_{ph}, and the experimental determination of $\tau_{e\text{–}ph}$ as in fast optical reflectivity changes measurements allow us to solve numerically the 2-T equations obtaining information about the involved dynamics.

The role of the superconducting material is crucial, since it influences drastically the electron-phonon scattering time, the heath capacity, and the escape rate for phonons. NbN and $YBa_2Cu_3O_{7-x}$ (YBCO) have been demonstrated to be good choices as superconducting materials for bridge-type superconducting photodetectors, as they are characterized by the overall picosecond photoresponse [3,4].

Besides simple metals or compounds, heterogeneous structures formed by a superconductor (S) and a normal metal (N) in good electrical contact offer an interesting option for the optimization of the ultrafast carrier dynamics regime. According to the physics of the proximity effect, two materials that form a bilayer influence each other near their interface on a spatial scale on the order of their coherence lengths-[5]. However, because of the small value of the optical penetration depth $\alpha < 50$ nm for metals at visible-light wavelengths (400-900 nm), optical experiments should sense electronic properties of only one (N) of the proximized layers, far from the interface where the major effect takes place in terms of spatial modification of the order parameter. Weak-ferromagnet/superconductor (F/S) bilayers are very interesting, since for these hybrids the coherence length in F, ξ_F, is on the order of few nm due to the presence of the magnetic exchange energy, and it can be modulated by varying the thickness of the F layer in the α range.

Time-resolved transient pump–probe spectroscopy allows us to investigate the electron-phonon relaxation times of proximized F/S nanobilayers as a function of F thickness and temperature. This characterization is useful for selecting structures with ultra-fast carrier dynamic for fast photodetectors. In this paper we focused our attention on both low- and high-critical-temperature superconductors (LTS and HTS) such as Nb and YBCO, well characterized in terms of the dynamics of the relaxation process [6,7], while for F we have chosen weak-ferromagnetic alloy $Ni_{0.48}Cu_{0.52}$.

II. EXPERIMENTAL

A. Sample Fabrication

Thin Nb films were deposited by using a dedicated DC magnetron sputtering system. 70-nm-thick, base Nb layers were sputtered at a base pressure of $1.3\text{x}10^{-5}$ Pa on chemically cleaned Corning glass substrates. The sputtering power and the deposition rate were 700 W and 2.2 nm/s. For the $Ni_{0.48}Cu_{0.52}$ deposition, samples were inserted inside another vacuum system, where their surface was first cleaned for 30 s using ion beam etching at a rate of about 0.2 nm/s. Afterwards, $Ni_{0.48}Cu_{0.52}$ films were deposited at a rate of 1.5 nm/s and a sputtering power of 200 W. The thickness of $Ni_{0.48}Cu0_{.52}$ ranged from 6nm to 21 nm. Niobium films were polycrystalline, while $Ni_{0.48}Cu_{0.52}$ either amorphous, or polycrystalline with the grain size < 1 nm. Further information about the physical characterization of $Ni_{0.48}Cu_{0.52}$ films can be found elsewhere [8]. Their coherence length was estimated to be ξ_F= 24 nm [9].

The 100-nm thick c-axis YBCO films were deposited by DC magnetron sputtering on $SrTiO_3$ substrates at $T = 950$ K. The sputtering power and the deposition rate were 100 W and 3 nm/s. Subsequently, the film was annealed at T=500 K, and covered by an Au buffer layer (about 20 nm), deposited by sputtering technique to reduce the out-diffusion of O_2 from the superconducting film. The roughness of the YBCO film was estimated to be lower than 2 nm. Afterwards, $Ni_{0.48}Cu_{0.52}$ films were deposited in a dedicated system as described above. The superconducting transition temperatures were T_C = 8.9 K and T_C = 89 K for pure Nb and YBCO films, respectively.

B. Pump and Probe Spectroscopy

Femtosecond pump–probe spectroscopy experiments were performed using a commercial, mode-locked, Ti:sapphire laser, with 100 fs pulses at the 810 nm wavelength with a repetition rate of 80 MHz. The pump and probe beams are cross polarized to eliminate coherent artifacts due to the interference of the two beams. The samples are mounted on a cold finger in a temperature-controlled liquid-helium continuous flow optical cryostat operating down to 5K. A schematic of the experimental set-up is shown in Figure 1. Both pump and probe beams are focused down to 30 μm diameter spot onto the sample. The pump-probe average power ratios were set at 10:1 for Nb and 3:1 for YBCO. The fluences were set at about 100 $\mu J/cm^2$ and 30 $\mu J/cm^2$, values which minimize the optical heating while assuring good signal-to-noise ratio. The reflectivity signal is measured from the probe beam time-delayed with respect to the pump. The reflectivity change as a function of the time delay between the pump and the probe beams is directly related to the relaxation processes of excited carriers. In particular, the hot electrons thermalize first with other electrons through electron-electron relaxation on a time scale shorter than the pump pulse width. Subsequently, they relax their energy by electron–phonon scattering. Finally, the bolometric lattice cooling process takes place on a time scale of the order of ns. Therefore, measuring the reflectivity change in the ps range provides a direct probe of the electron-phonon relaxation processes which tend to restore the equilibrium between the electron and phonon subsystems.

The optical penetration depth of $Ni_{0.48}Cu_{0.52}$ films was measured to be α = 10.6 nm at 810-nm.

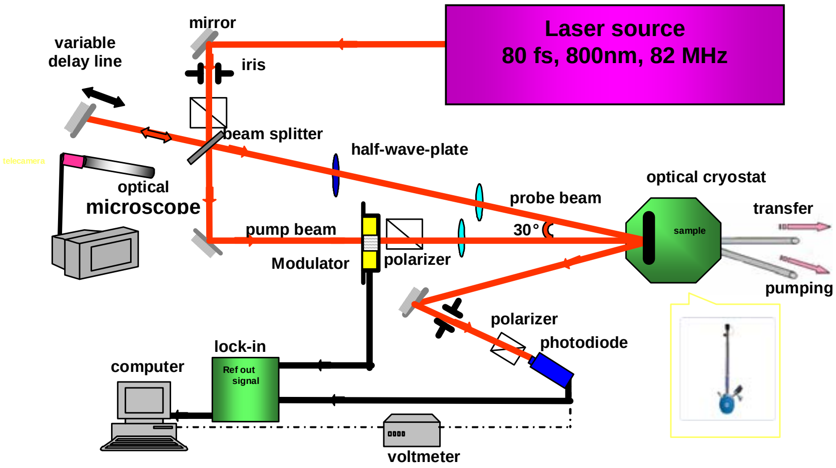

Fig. 1. Experimental set-up for pump and probe spectroscopy

III. RESULTS AND DISCUSSION

Pump–probe experiments were performed in a temperature range between 5 K and room temperature. Figure 2 shows the time-resolved, normalized optical reflectivity, Δ*R*/*R*, signals collected at 6 K for NiCu, Nb, and two $Ni_{0.48}Cu0_{.52}$/Nb bilayers with different thicknesses of $Ni_{0.48}Cu_{0.52}$. The waveforms are representive for measurements in the whole temperature range.

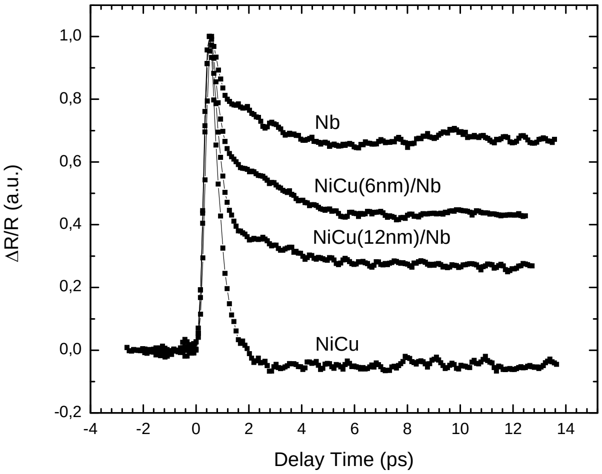

Fig. 2. Normalized optical reflectivity signals as detected by the pump-probe measurements for fabricated Nb/ $Ni_{0.48}Cu_{0.52}$ samples at $T = 6$K .

The reflectivity time spectra were fitted by using a two-exponential fitting formula with two different decay channels characterized by $\tau_{\rm fast}$ and $\tau_{\rm slow}$ times respectively. The fast relaxation time, subpicosecond in duration, corresponds to electron–Debye-phonon interaction of highly excited electrons. In the superconducting state, it leads to the accumulation of quasiparticles just above the superconducting energy gap. The slow relaxation time on the order of a few picoseconds refers to inelastic electron–acoustic-phonon scattering and Cooper pair recombination. Finally, we observed a plateau, related to the bolometric phonon escape, which decayed on a time scale of hundreds of picoseconds.

The photoresponse signal in Nb samples is dominated by the slow bolometric decay, while the pure $Ni_{0.48}Cu_{0.52}$ is like a 0.5-ps-wide spike. F/S bilayers exhibit responses which are intermediate between the pure Nb and $Ni_{0.48}Cu_{0.52}$, since the plateau level decreases when increasing the $Ni_{0.48}Cu_{0.52}$ thickness. Probably, the presence of the thicker F overlayer reduces the breaking of Cooper pairs in the underlaying Nb layer, and makes less effective the “phonon bottleneck” effect responsible for the long time decay in reflectivity signals for photoexcited homogeneous superconducting films. The strongly suppressed bolometric plateau in F/S bilayers makes them very attractive for fast optical superconducting detectors.

The low-temperature $\tau_{\rm fast}$ varies overall between ~0.18 ps (Nb film) to ~0.32 ps ($Ni_{0.48}Cu0_{.52}$ (21nm)/Nb bilayer), but for each sample the dependence is rather flat and no special features can be observed. At room-temperature $\tau_{\rm fast}$ is longer and more than twice that of the averaged low-temperature value. The $\tau_{\rm slow}$ time varies from ~2.5 ps (Nb film) to ~5.2

ps ($Ni_{0.48}Cu0_{.52}$(12nm)/Nb bilayer) in the whole investigated temperature range. In the τ_{slow} (T) case, we observed a rich structure with peak magnitudes well above our experimental error level, but were unable to associate this structure with any expected temperature dependences such as, e.g., divergence corresponding to the T_c of the F/S bilayer. Figure 3 shows the normalized reflectivity change $\Delta R/R$ as a function of time delay for a NiCu(20nm)/Au(20nm)/YBCO(100 nm). It is compared to photoresponse of a pure YBCO (100nm) film. The superconducting transition temperature was $T_c = 45$ K. The presence of the ferromagnetic layer causes faster relaxation times as evidenced by the fitted curves (red lines in Figure 3) and summarized in Table I.

The F layer slightly reduces also the bolometric component of the signal, according to the physical mechanism discussed above. Measurements on new samples with different NiCu thicknesses are still in progress: they should allow us to study also the role of the Au film used as a buffer layer. The presence of the Au overlayer can help also the fabrication process of nanosized YBCO based devices that still represent a challenge.

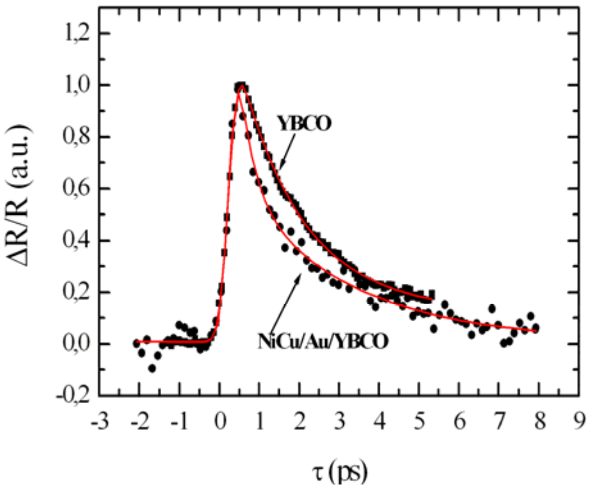

Fig. 3. Normalized **o**ptical reflectivity signals as detected by the pump-probe measurements for bilayer samples fabricated with YBCO at $T = 15$K .

Table I. τ_{fast} and τ_{slow} extracted by a two-exponential fit of the decay part of the waveforms at low temperature.

Parameter/Sample	τ_{fast} (ps)	τ_{slow} (ps)
YBCO	1.32	2.7
NiCu/Au/YBCO	0.35	2.8
Nb	0.18	2.5
NiCu(12nm)/Nb	0.26	5.2

IV. CONCLUSIONS

We performed femtosecond optical pump-probe measurements of proximized F/S structures formed by a ferromagnet ($Ni_{0.5}Cu_{0.5}$) and both LTS and HTS superconductor (Nb and YBCO, respectively). The presence of a thin F overlayer on the top of the S film reduces the slow bolometric component of the photoresponse. Moreover, a reduction of the fast decay time, related to the electron-phonon scattering, is observed in the case of YBCO based heterostructures. These properties of F/S bilayers are promising for future development of ultrafast superconducting optical detectors based on F/S structures.

ACKNOWLEDGMENTS

This work has been partially supported by MIUR, PRIN 2006, under the project "Macroscopic Quantum Systems- Fundamental Aspects and Applications of Non Conventional Josephson Structures"

REFERENCES

[1] G. M. Éliashberg, *Sov. Phys*.-JETP **11**, 696-702 (1960).
[2] M. L. Kaganov, I. M. Lifshitz, and L. V. Tanatarov, *Sov. Phys.-JETP* **4**, 173-178 (1957).
[3] K. S. Il'in, M. Lindgren, M. Currie, , S. I. Cherednichenko, and E. M. Gershenzon, *Appl. Phys. Lett*. **76**, 2752-2754 (2000).
[4] C. Williams, Y. Xu, R. Adam, M. Darula, O. Harnack, J. Scherbel, M. Siegel, F. A. Hegmann, and R. Sobolewski, *IEEE Trans. Appl. Supercon*. **11**, 578-580 (2001).
[5] A.A. Golubov, E.P. Houwman, J.G. Gijsbertsen, V.M. Krasnov, M. Yu Kupriyanov, J. Flokstra, H. Rogalla, *Phys. Rev*. B **51**, 1073-1089 (1995).
[6] M. Mihailidi, Q. Xing, K.M. Yoo and R.R. Alfano, *SPIE Proc.* **1677**, 108-115 (1992).
[7] T. Gong, L.X. Zheng, W. Xiong, W. Kula, Y. Kostoulas, R. Sobolewski, P.M. Fauchet, *Phys. Rev*. B **47**, 14495-14502 (1993).
[8] T. Taneda, G.P.Pepe, L. Parlato, A. A. Golubov and R. Sobolewski, *Phys. Rev*. B **75**, 174507-174513 (2007).
[9] G. P. Pepe, R. Latempa, L. Parlato, A. Ruotolo, G. Ausanio, G. Peluso, A. Barone, A. A. Golubov, Ya. V. Fominov, and M. Yu. Kupriyanov, *Phys. Rev*. B **73**, 054506-054514 (2006).